Neuron, Vol. 33, 779–788, February 28, 2002, Copyright ©2002 by Cell Press

Contributions of Receptor Desensitization and Saturation to Plasticity at the Retinogeniculate Synapse

Chinfei Chen,[1,2,3,4] Dawn M. Blitz,[1,4] and Wade G. Regehr[1]
[1]Department of Neurobiology
Harvard Medical School
[2]Division of Neuroscience
The Children's Hospital
Harvard Medical School
Boston, Massachusetts 02115

Summary

The retinogeniculate synapse conveys visual information from the retina to thalamic relay neurons. Here, we examine the mechanisms of short-term plasticity that can influence transmission at this connection in mouse brain slices. Our studies show that synaptic strength is modified by physiological activity patterns due to marked depression at high frequencies. Postsynaptic mechanisms of plasticity make prominent contributions to this synaptic depression. During trains of retinal input stimulation, receptor desensitization attenuates the AMPA EPSC while the NMDA EPSC saturates. This differential plasticity may help explain the distinct roles of these receptors in shaping the relay neuron response to visual stimulation with the AMPA component being important for transient responses, while sustained high frequency responses rely more on the NMDA component.

Introduction

Visual information encoded in the firing patterns of retinal ganglion cells is transmitted to the cortex via the retinogeniculate synapse in the dorsal lateral geniculate nucleus (LGN). Simultaneous in vivo recordings of retinal ganglion cells and their target relay neurons in the LGN demonstrate that the firing patterns of the postsynaptic neuron can differ significantly from those of the presynaptic cell, indicating that the LGN is not a simple relay station (Cleland and Lee, 1985; Mastronarde, 1992; Rowe and Fischer, 2001; Usrey et al., 1998). In vivo and in vitro studies of the thalamocortical circuitry show that responses of relay neurons to visual stimulation can be modulated by several processes (Guido and Lu, 1995; McCormick and Bal, 1994; Sherman and Guillery, 1996; Steriade et al., 1997). Both the inhibitory feedback circuitry intrinsic to the thalamus, as well as corticothalamic inputs, can influence the firing of relay neurons. Brainstem inputs that alter the membrane properties of relay neurons can also modify the response of postsynaptic cells to retinal ganglion cell activity. Much less is known, however, regarding how activity-dependent mechanisms of plasticity at the retinogeniculate connection can influence the response of relay neurons.

Short-term synaptic plasticity is likely to affect how information is transmitted from the retina to the visual cortex. In mature animals, each relay cell is contacted by a small number of powerful excitatory inputs mediated by AMPA and NMDA receptors (AMPAR and NMDAR) (Chen and Regehr, 2000; Ramoa and McCormick, 1994; Turner et al., 1994). Although AMPAR contribute significantly to the transient responses of relay neurons, NMDAR appear to be more important in mediating the sustained responses of relay neurons to repetitive, high-frequency optic tract stimulation (Turner et al., 1994) or to visual stimulation (Kwon et al., 1991; Sillito et al., 1990). The inability of the AMPAR component to maintain efficacy during sustained activation and the importance of NMDA receptors in mediating sustained responses is not well understood.

A variety of mechanisms can give rise to short-term synaptic plasticity (Magleby, 1987; Zucker, 1989). Two commonly observed presynaptic mechanisms include facilitation, where increases in presynaptic residual calcium from recent activity results in enhancement of neurotransmitter release, and depression, which may reflect depletion of release-ready vesicles (Zucker, 1999). Postsynaptic mechanisms, including receptor desensitization, can also rapidly alter synaptic strength, although there are fewer reports documenting this in the CNS (Trussell, 1999). At the retinogeniculate synapse, previous in vitro studies have shown that synaptic depression occurs in response to pairs of pulses (Chen and Regehr, 2000; Turner and Salt, 1998). However, the mechanisms that underlie this synaptic behavior and their contributions to regulating the response of relay neurons are unclear.

Here, we study short-term plasticity at the retinogeniculate synapse in mouse brain slices. These experiments were conducted under conditions where synaptic properties could be studied without contributions from cortical feedback, brainstem modulation, inhibitory circuitry, and voltage-gated conductances of relay neurons. Pairs of closely spaced retinal input stimuli evoke AMPAR and NMDAR excitatory postsynaptic currents (EPSCs) that depress. Recovery from depression for both the AMPA and NMDA receptor types can be approximated by fast and slow time constants. The slow phase of recovery is similar for both AMPA and NMDA components, consistent with a presynaptic mechanism of depression. The fast phase of recovery, which is more pronounced for the AMPA component, reflects a significant contribution from postsynaptic mechanisms, including AMPAR desensitization and NMDAR saturation. These mechanisms dynamically regulate synaptic strength during physiological stimulus trains. The relative importance of NMDAR and AMPAR components is altered during such trains by differential plasticity of these components and by contrasting properties of the receptors. Thus, mechanisms controlling short-term synaptic plasticity at the retinogeniculate connection may help shape relay neuron responses to varying visual stimuli.

[3]Correspondence: chinfei.chen@tch.harvard.edu
[4]These authors contributed equally to this work.

Results

Short-term plasticity was examined at single fiber, retinogeniculate connections in parasagittal brain slices from postnatal day (P)25–P32 mice (Chen and Regehr, 2000). Relay neurons receive a small number of strong retinal inputs in these young adult mice, and synaptic responses to single fiber stimulation can be studied (see Experimental Procedures). The response of the excitatory retinogeniculate synapse was isolated by blocking inhibitory transmission with the $GABA_A$ antagonist bicuculline and by cutting the connections between the LGN and cortex. Moreover, synaptic currents are readily voltage clamped because geniculate cells are electrically compact and retinal inputs contact the proximal dendrites of geniculate neurons (Wilson et al., 1984). In these experimental conditions, brainstem modulation of intrinsic voltage-gated conductances in relay neurons do not contribute to the synaptic response.

Paired-Pulse Plasticity at the Retinogeniculate Synapse

To identify mechanisms of short-term plasticity that are important at the retinogeniculate synapse, we initially studied the response to pairs of stimuli. Both NMDAR and AMPAR components of the excitatory postsynaptic current (EPSC) can be monitored at a holding potential of +40 mV (Figure 1A). The outward current consists of the rapidly activating AMPAR component and the slower NMDAR component that decay with time constants of 2–3 ms and ~90 ms, respectively (Chen and Regehr, 2000). Activation of a retinal input with two stimuli separated by 100 ms leads to synaptic depression, and the amplitude of the second EPSC (A2) is smaller than that of the first EPSC (A1).

Differences in the depression of the AMPAR and NMDAR components of the synaptic current are apparent in the EPSC response to pairs of pulses. The lower panel of Figure 1A shows the superimposed EPSCs evoked by pairs of stimuli with interstimulus intervals (ISIs) varying from 10 to 200 ms. The relative proportion of the rapidly and slowly decaying components of the synaptic current changes with ISI. AMPAR and NMDAR contributions to the second EPSC are similar in size for an ISI of 10 ms, but the AMPAR component is larger than the NMDAR for an ISI of 200 ms.

To further elucidate the differences in synaptic depression of the AMPAR and NMDAR currents, we examined each component in isolation. In the presence of the NMDAR antagonist, 3-([*R*-]2-carboxypiperazine-4-yl)-propyl-1-phosphonic acid ([CCP]; 5 μM), the AMPAR current depressed to approximately 25% of the initial current for an ISI of 10 ms (Figure 1B, top). In contrast, when the NMDAR EPSC was isolated by inhibiting the AMPAR component with 2,3-Dioxo-6-nitro-1,2,3,4-tetrahydrobenzo[f]quinoxaline-7-sulphonamide disodium ([NBQX], 5 or 10 μM), synaptic depression is significantly less for an ISI of 10 ms (~50%; Figure 1B, bottom). To quantify the recovery of each component, we plotted the percent ratio of the peak amplitude of the second to first EPSC as a function of the ISI. Figure 1C (left) shows the summary of the changes in the paired-pulse ratio for the AMPAR (circles) and NMDAR (squares).

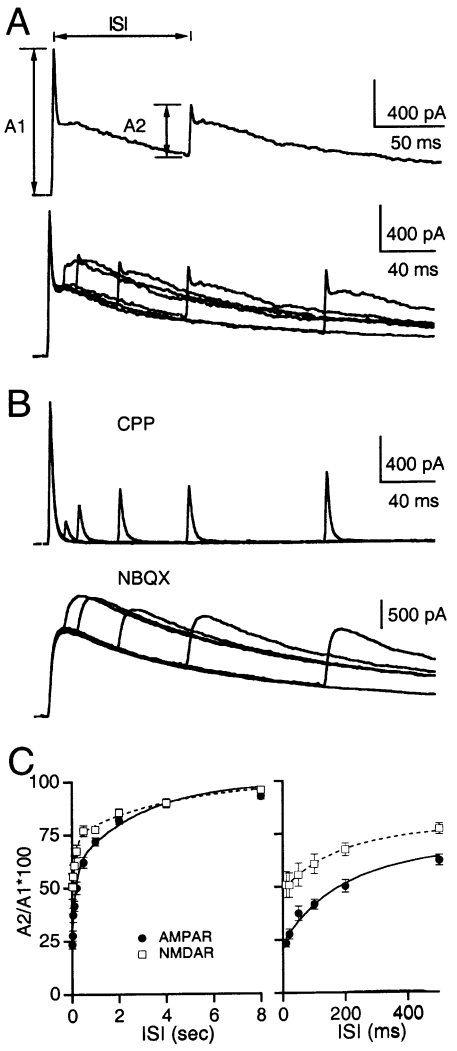

Figure 1. Paired-Pulse Plasticity at the Retinogeniculate Synapse

(A) The response to two stimuli separated by varying ISI was recorded at a holding potential of +40 mV to examine both the NMDAR and AMPAR components. A1 and A2 are the peak amplitudes of the first and second EPSC, respectively. ISI = 100 ms (top). Superimposed pairs of EPSCs separated by ISIs varying from 10 to 200 ms (bottom).

(B) Isolation of the AMPAR (top) and NMDAR (bottom) components of the synaptic current with bath application of 5 μM CPP and 5 μM NBQX, respectively. NMDA currents are obtained from a different experiment than in (A).

(C) The average ratio of the second to first EPSC as a function of ISI for AMPAR (circles, n = 10 cells) and NMDAR (squares, n = 9 cells). An expanded time course is shown on the right. Data represent the mean ± SEM and could be fit with a double exponential function, $100 + C1 \times \exp(-C2 \times x) + C3 \times \exp(-C4 \times x)$, where the constants C1, C2, C3, and C4 were −26.0, 0.25, −25.4, and 6.1 and −40.7, 0.35, −35.8, and 6.12 for the AMPAR (solid line) and NMDAR (dashed line), respectively. The peak EPSC amplitudes were measured in isolation in the presence of either CPP or NBQX. Bath temperature: 24°C–26°C.

Both glutamate receptor types recovered from depression with a time course that can be approximated by a double exponential (Figure 1C, lines). The slow component of recovery, best illustrated between ISI 2–8 s (Figure 1C, left), was similar for the AMPAR and NMDAR

components. However, for brief ISIs, there were significant differences in short-term plasticity (Figure 1C, right). Although the time course of the fast component of recovery was similar, the amplitude of the component was greater for the NMDAR when compared to that of the AMPAR.

The Role of Postsynaptic AMPAR Desensitization

There are many possible mechanisms that can underlie depression at the retinogeniculate connection. In addition to presynaptic processes that may reduce the number of vesicles available for release on the second stimulus of a closely spaced pair of pulses, postsynaptic mechanisms, such as receptor desensitization, could play a role. In light of the differences in synaptic depression of the glutamate receptor classes, we examined the possible role of postsynaptic AMPAR desensitization in depression of this synapse.

The effect of cyclothiazide (CTZ), a compound that inhibits desensitization of the AMPAR, on pairs of retinal input stimuli is shown in Figure 2A (left). The AMPAR response at +40 mV to two stimuli separated by 100 ms is shown before (Figure 2A, bold lines) and during (thin line) bath application of CTZ (75 μM). This compound increased the peak amplitude and time course of decay of both EPSCs. Moreover, CTZ decreased the degree of synaptic depression. In addition to inhibiting AMPAR desensitization, at other synapses CTZ can alter vesicular release through a presynaptic mechanism (Bellingham and Walmsley, 1999; Diamond and Jahr, 1995). To determine if changes in the release probability contributed to the relief of synaptic depression by CTZ, we examined the effects of CTZ on the NMDAR component of synaptic depression. If CTZ acts through a presynaptic mechanism, then it should also affect pairs of NMDAR EPSCs. Figure 2A (right) demonstrates that at concentrations up to 100 μM, CTZ does not alter the NMDAR paired-pulse ratio (n = 3 cells, percent of A2/A1 for ISI 100 ms: 0 μM CTZ, 59.5% ± 5.9%; 100 μM CTZ, 56.2% ± 5.5%; SEM). Thus, at concentrations less than 100 μM, CTZ is a useful tool for clarifying the role of AMPAR desensitization at the retinogeniculate synapse.

CTZ alters the time course of recovery from depression of the AMPAR component. This is apparent in the traces of pairs of EPSCs before (Figure 2B, top) and during bath application of 75 μM CTZ (Figure 2B, bottom). The slow component of recovery is not significantly affected by 20 μM (squares), 50 μM (diamonds), or 75 μM (triangles) CTZ (Figure 2C, left). However, the magnitude of the fast phase of recovery is reduced in a dose-dependent manner by CTZ (Figure 2C, right). Thus, the fast component of recovery from depression of the AMPAR current reflects postsynaptic AMPAR desensitization.

Mechanisms Underlying Depression of NMDAR Currents

It appears that AMPAR desensitization cannot account fully for the difference in depression of the NMDAR and AMPAR currents. This is apparent when Figure 1C is compared to Figure 2C, which shows that when desensitization is reduced by CTZ, the AMPAR current is less depressed at short time intervals than the NMDA current. To further understand the mechanisms that underlie the fast component of recovery from depression of the NMDAR current, we examined whether the rapidly recovering phase of NMDA EPSC depression also reflects a postsynaptic mechanism. One possibility is partial saturation of NMDA receptors, resulting in fewer receptors available to respond to a second pulse of glutamate. We tested this by using NMDAR antagonists with different kinetics, which have proven useful in examining NMDAR saturation previously (Clements et al., 1992; Wang, 2000).

The rationale for using NMDAR antagonists of low affinity with fast kinetics and of high affinity with slow kinetics is illustrated in Figure 3A. In the extreme case of complete saturation, all NMDARs would bind glutamate on the first pulse and no receptors would be available for a second stimulus with a sufficiently short ISI. This would result in a failure to evoke a second EPSC

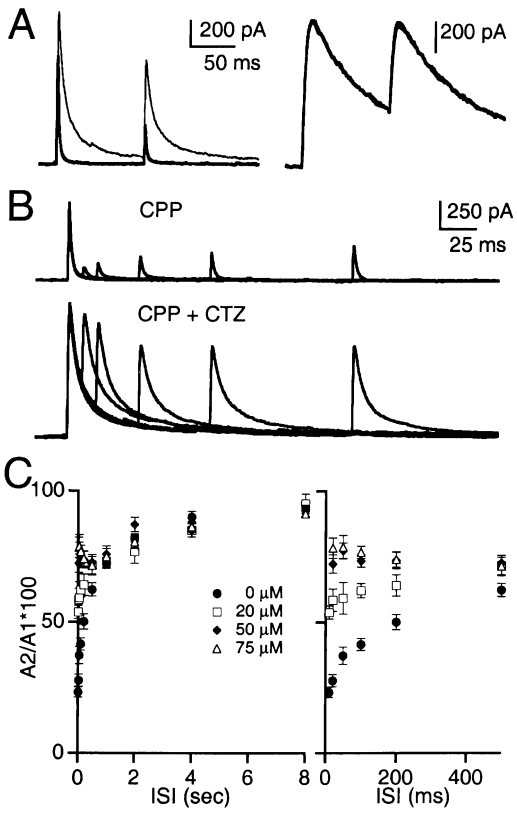

Figure 2. CTZ Relieves the Fast Component of AMPAR Synaptic Depression

(A) Left, the response of the AMPAR EPSC to a pair of stimuli separated by 100 ms is shown before (bold trace) and during (thin trace) bath application of CTZ (75 μM). Right, the NMDAR paired-pulse ratio (control, bold trace) remains unchanged in the presence of 100 μM CTZ (thin trace). (B) Superimposed pairs of AMPAR EPSCs with varying ISI are shown before (top) and during (bottom) bath application of CTZ. The effects of increasing concentrations of CTZ (0 μM (circles, n = 10 cells), 20 μM (squares, n = 5 cells), 50 μM (diamonds, n = 5 cells), and 75 μM (triangles, n = 6 cells) on the paired-pulse ratio is shown in (C). Data represents the mean ± SEM The fast component of depression is resolved on an expanded time scale on the right. EPSC traces are the average of three to five trials. Bath temperature: 24°C–26°C.

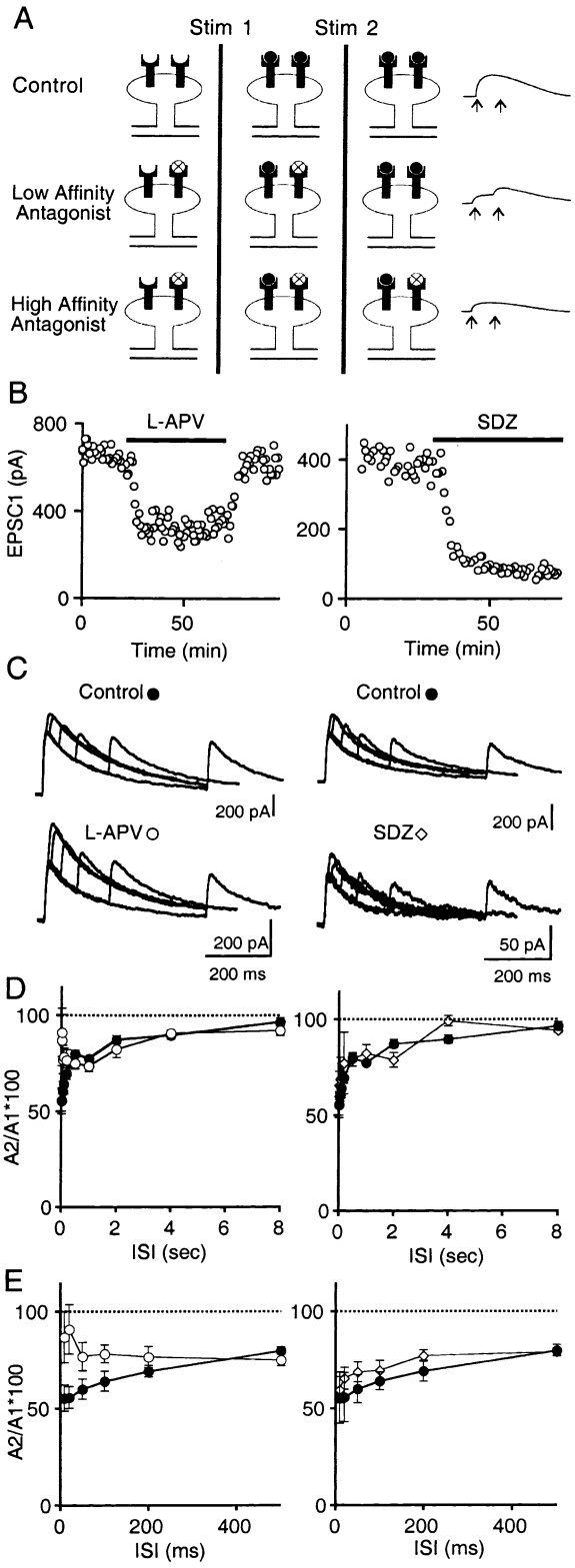

Figure 3. A Low-Affinity NMDAR Antagonist Decreases the Rapidly Recovering Phase of Depression of the NMDA EPSC

(A) A schematic illustrates the possible contribution of NMDAR saturation to paired-pulse plasticity. Postsynaptic NMDAR are shown in the unbound state, bound with glutamate (black circles), or bound with antagonist (circles with X). The EPSC response to a pair of stimulation (indicated by arrows) is shown for each condition on the right. (B) Initial EPSC amplitude is plotted against time during control conditions and during application of NMDAR antagonists indicated by the black bars. (C) NMDA EPSCs with paired-pulse intervals of 10, 20, 50, 100, 200, and 500 ms in control conditions and during L-APV or SDZ 220-581 application. The first EPSC in antagonist has been normalized to the corresponding first control EPSC. Traces are the average of five consecutive trials. (D) Average data (mean ± SEM) for control paired-pulse plasticity (closed circles, n = 7 cells) and during L-APV application (open circles, n = 5 cells) or SDZ 220-581 application (open diamonds, n = 3 cells) is plotted for the entire range of ISIs and (E) for only the six shortest paired-pulse intervals. Bath temperature: 24°C–26°C.

(Figure 3A, top row). When a low-affinity antagonist blocks a subset of NMDARs, glutamate activates available receptors eliciting a smaller EPSC than the control. However, due to a faster dissociation rate of the antagonist, some receptors become available for a second glutamate pulse to elicit another EPSC (Figure 3A, middle row). In contrast, if a high-affinity antagonist blocks the same percentage of NMDARs, both antagonist and glutamate will remain bound after the first pulse, providing no available receptors for the second stimulus (Figure 3A, bottom row). The same reasoning applies even when receptor saturation is not complete and predicts that if NMDAR saturation is playing a role, the high-affinity antagonist should not alter the plasticity, whereas the low-affinity one should decrease the depression.

Using this experimental paradigm, we found that a low-affinity NMDAR antagonist did alter paired-pulse plasticity while a high-affinity one did not. The low-affinity NMDAR antagonist L-APV (400 μM) (Olverman et al., 1988) elicited a readily reversible decrease in initial EPSC amplitude (Figure 3B, left; inhibition by 77.5% ± 3.1%, SEM, n = 5 cells). SDZ 220-581 (50 nM), a high-affinity NMDAR antagonist (Urwyler et al., 1996), elicited a decrease in initial EPSC amplitude (Figure 3B, right; inhibition by 74.3% ± 5.8%, SEM, n = 3 cells). This inhibition was not readily reversible (data not shown). Paired-pulse depression still occurred in the presence of these antagonists. However, normalizing the initial EPSC in antagonist to the corresponding initial control EPSC demonstrates that L-APV decreased the depression at short ISIs, while SDZ 220-581 did not change the plasticity (Figure 3C). This was the case for all cells we examined, as indicated in the average plots of paired-pulse plasticity (Figures 3D and 3E). L-APV decreased the amount of depression at ISIs of 10–100 ms, while at longer ISIs (0.2–8 s), there was little difference in paired-pulse plasticity (Figures 3D and 3E). During SDZ 220-581 application, however, there was no difference from control across the entire range of ISIs.

Comparison of Synaptic Depression When Desensitization and Saturation Are Minimized

Differences between synaptic depression of the AMPAR and NMDAR EPSCs can be attributed to postsynaptic receptor desensitization and saturation. This is apparent when depression is compared for the two receptor classes when the effects of desensitization of the AMPAR are removed with CTZ, and the effects of NMDAR saturation are minimized by a low-affinity an-

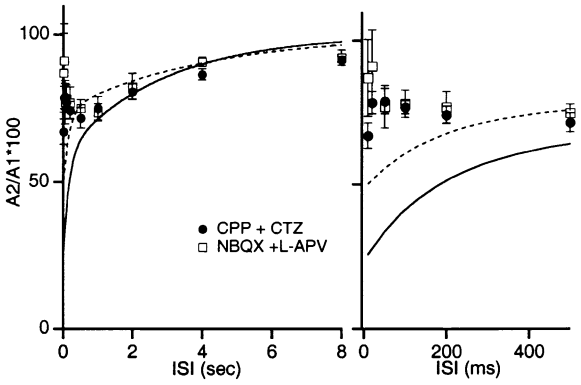

Figure 4. Similarity of Paired-Pulse Ratio When Desensitization and Saturation Are Reduced

The paired-pulse ratio for the AMPAR in the presence of CTZ (75 μM, circles, n = 6 cells) and NMDAR in the presence of L-APV (squares, n = 5 cells) is plotted as a function of the interstimulus interval (ISI). Expanded time scale shown on the right. Lines represent the fits of the control AMPAR and NMDAR data from Figure 1C. Data represent the mean ± SEM. Bath temperature: 24°C–26°C.

tagonist (Figure 4). In these conditions, the magnitude of depression is similar for the two classes of receptors.

Contributions of Short-Term Synaptic Plasticity during Physiological Stimulation

We examined whether synaptic plasticity was important under physiological conditions by examining the response of the retinogeniculate synapse to a train of stimuli designed to mimic the firing pattern recorded from a mouse retinal ganglion cell in response to a flash of light (see Experimental Procedures). Synaptic currents were recorded at 34°C–37°C. We found that the amplitude of both AMPAR and NMDAR EPSCs varied more than 5-fold during stimulation (Figure 5A). The EPSC amplitude depends on the recent history of the synapse for both receptor types. For example, the EPSC evoked by the second stimulus is ~15% to ~25% of that evoked by the first because it follows the first by just 7 ms. In contrast, after a long quiescent period (87 ms), the response to the seventh action potential elicits a response that is 60%–65% of the first EPSC. To quantify the synaptic response to trains for the representative examples shown, the peak amplitude of each AMPAR or NMDAR EPSC was normalized to the first EPSC amplitude (A/A1) (Figure 5A, bottom). The average responses and standard deviations are plotted as a function of time from the initial stimulus for five consecutive trials to illustrate the reproducibility of these synaptic responses.

A summary of the responses of many cells illustrates that the incremental increases in NMDAR (triangles) and AMPAR (circles) EPSCs are strongly attenuated during trains (Figure 5B). However, the total peak NMDAR current does not exhibit this degree of attenuation because the long duration of each individual EPSC response leads to summation of their currents (Figure 5C).

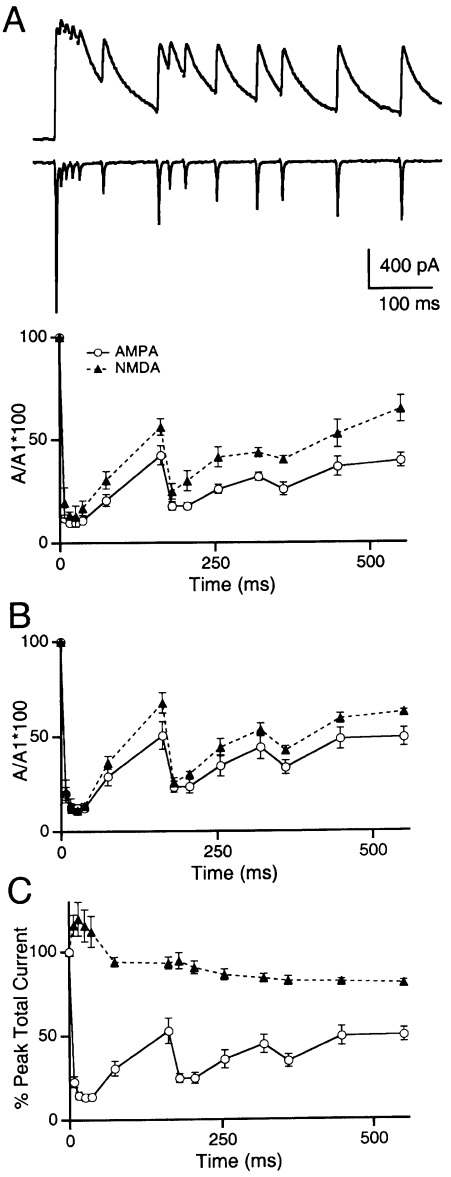

Figure 5. Response to Realistic Spike Trains at the Retinogeniculate Synapse

(A) Representative traces of the NMDAR (top) and AMPAR (middle) EPSCs evoked from a train of retinal input stimulation. NMDAR and AMPAR currents were recorded from different cells at a holding potential of +40 mV and –70 mV and in the presence of NBQX and CPP, respectively. Scale bars apply to both currents. (Bottom) The trial-to-trial variability of the synaptic response for the two currents shown above are plotted below as the average relative peak amplitude of each EPSC in the train versus the time from the first EPSC of the train (mean ± SD, five trials each). A1 and A are the peak amplitude of the first EPSC and the EPSC at a given time, respectively. The average relative incremental peak (B) and total peak (C) current amplitudes in response to each stimulus of the train are plotted as a function of time (mean ± SEM) for the NMDAR (triangles, n = 5 cells) and AMPAR (circles, n = 4 cells) EPSCs. Bath temperature: 34°C–37°C.

The Role of AMPAR Desensitization in the Synaptic Response to Physiological Trains

We evaluated the contributions of AMPAR desensitization to short-term plasticity of the retinogeniculate connection under more physiological conditions by studying the effects of CTZ on the synaptic response to trains at 34°C–37°C. Figure 6A shows an example of a response to a physiological pattern of stimuli before (top) and

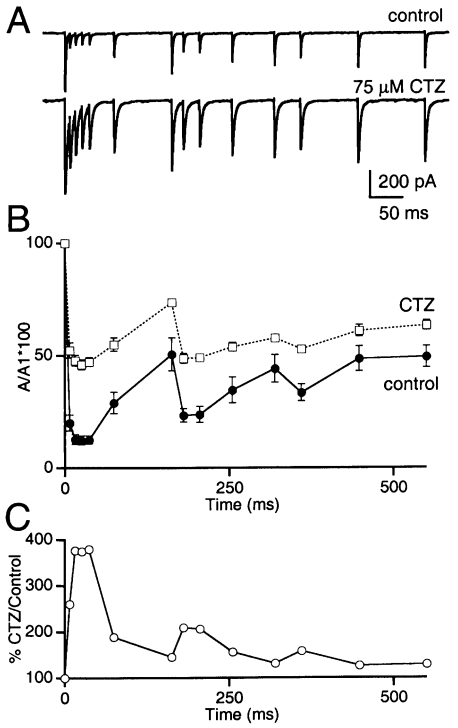

Figure 6. Desensitization Attenuates the Amplitude of AMPA EPSCs Evoked by Physiological Trains

(A) AMPAR responses to a train of stimuli are shown in control conditions and after bath application of 75 μM CTZ.

(B) The average incremental peak EPSC amplitude for each stimulus is normalized to the first EPSC in the train and plotted as a function of the time (mean ± SEM; control, circles, n = 4 cells; CTZ, squares, n = 4 cells).

(C) The relative enhancement of each EPSC in CTZ, calculated as a percent (relative weight in CTZ/relative weight in control) is plotted for each stimulus.

Bath temperature: 34°C–37°C.

during bath application of 75 μM CTZ (bottom). CTZ application results in an alteration in the relative strength of each EPSC in the train (Figure 6A). Changes in the strength of each EPSC in the presence of CTZ were reproducible from cell to cell, as illustrated in the summary plot of the relative peak amplitude of each EPSC in the train for control conditions (circles) and in the presence of CTZ (squares) (Figure 6B). To quantify the role of desensitization on the short-term plasticity of this synapse, the ratio of the relative weight of each EPSC in the presence of CTZ versus control conditions is plotted in Figure 6C. Inhibition of desensitization by CTZ enhances the strength of the synaptic response to the subsequent stimuli in a train relative to the first stimuli by 125%–380%, with the most prominent changes in relative strength occurring in response to high-frequency spikes. CTZ did not affect the relative strength of NMDA EPSCs in response to trains at 34°C–37°C (relative weight of fourth EPSC of train: 13.5% ± 1.6% in control, n = 3 cells versus 12.9% ± 1.5% in 75 μM CTZ, n = 3 cells).

The Role of NMDAR Saturation in the Synaptic Response to Physiological Trains

To examine whether NMDAR saturation might also be contributing to plasticity under more physiological conditions, we again used concentrations of L-APV (800 μM) and SDZ 220-581 (100 nM) that partially blocked NMDA EPSCs to a similar extent (Figure 7A). As for pairs of pulses at room temperature, partial NMDAR blockade with L-APV decreased depression during trains (Figures 7B and 7D). This was most pronounced during the early

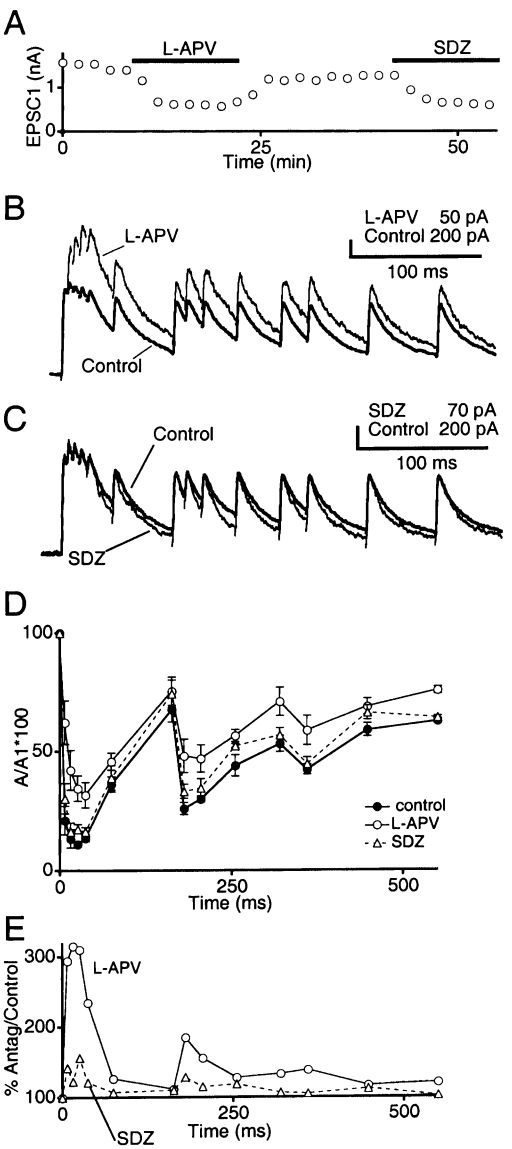

Figure 7. Saturation of the NMDAR Occurs during Realistic Trains

(A) Initial EPSC amplitude is plotted against time for control conditions and with partial NMDAR blockade by L-APV and SDZ 220-581 during a representative experiment.

(B and C) NMDA EPSCs in control conditions and in the presence of L-APV or SDZ 220-581. The antagonist traces have been scaled to normalize the first EPSC in antagonist to the corresponding first control EPSC. Traces are the average of five consecutive trials.

(D) Plot of the average incremental amplitude of subsequent EPSCs (mean ± SEM) normalized to the first in control conditions (closed circles, n = 5 cells) and after bath application of L-APV (open circles, n = 5 cells), and SDZ 220-581 (open triangles, n = 3 cells).

(E) Ratio of the percent change in EPSC amplitude during L-APV (open circles) or SDZ 220-581 (open triangles) application to percent change during control conditions.

Bath temperature: 34°C–37°C.

higher-frequency portion and less dramatic with longer ISIs later in the train. A similar NMDAR blockade by SDZ 220-581, however, did not alter plasticity during the train even during the higher-frequency segment (Figures 7C and 7D). In a plot of the ratio of the relative change during L-APV to that of control, it is evident that relative EPSC amplitude is increased more than 300% in L-APV during the first few stimuli (Figure 7E). SDZ 220-581 did not have this dramatic effect.

Discussion

We find that the strength of the retinogeniculate synapse is modified in an activity-dependent manner. This plasticity reflects, in part, presynaptic mechanisms of depression. In addition, a large component of synaptic plasticity also arises from postsynaptic processes. Our results show that AMPAR and NMDAR are differentially regulated. During bursts of afferent activity, receptor desensitization diminishes the AMPAR EPSC and receptor saturation attenuates the NMDAR EPSC. Thus, unlike many CNS synapses, the transmission of visual information from the retina to the brain relies upon synapses with prominent postsynaptic plasticity.

AMPAR Desensitization Contributes to Plasticity of the Retinogeniculate Synapse

Our studies show that AMPAR desensitization plays a prominent role in the response to physiological trains of stimulation at the retinogeniculate connection. Inhibition of desensitization with CTZ relieves a fast component of recovery from synaptic depression. During bursts of high-frequency activity, desensitization can attenuate the EPSC by 3- to 4-fold.

Interestingly, another connection where desensitization plays an important role in plasticity is also in a sensory pathway—the calyceal synapse between primary afferents and nucleus magnocellularis neurons in the chick auditory system (Otis et al., 1996a; Trussell et al., 1993). At that synapse, inhibitors of desensitization relieve synaptic depression to pairs of pulses and trains and increase the postsynaptic refractory period following synaptically driven action potentials (Brenowitz and Trussell, 2001; Raman et al., 1994). Perhaps desensitization is a feature of the synapse that is useful where timing is important, as in both the visual and auditory systems (Trussell, 1997, 1999; Usrey and Reid, 1999).

Although all AMPA receptors desensitize, this postsynaptic mechanism does not contribute significantly to synaptic plasticity at most synapses that have been studied (Chen et al., 1999; Dittman and Regehr, 1998; Hestrin, 1992; Hjelmstad et al., 1999). Previous studies suggest that the importance of AMPAR desensitization to short-term plasticity at a given connection is likely dictated by the morphological structure of the specific synapse, as well as the probability of release and the time course of transmitter clearance (Barbour and Hausser, 1997; Kinney et al., 1997; Oleskevich et al., 2000; Otis et al., 1996b; Silver et al., 1996; Trussell, 1999; Walmsley et al., 1998). In the case of both the retinogeniculate and chick calyceal synapses, prominent presynaptic depression suggests that there is a high probability of release. Moreover, both synapses have many closely spaced release sites defined as the contact between a presynaptic active zone and a postsynaptic receptor cluster that are not well isolated from one another (Cant and Morest, 1979; Hamos et al., 1987; Lenn and Reese, 1966; Parks, 1981). In addition, glial sheaths that encompass aggregates of some synaptic contacts onto the geniculate neuron may contribute to prominent AMPAR desensitization by allowing glutamate to pool (Famiglietti and Peters, 1972; Hamos et al., 1985).

At most other CNS synapses, desensitization does not affect short-term plasticity (Chen et al., 1999; Dittman and Regehr, 1998; Hestrin, 1992; Hjelmstad et al., 1999) because there is limited cross-talk between individual release sites, and the probability of release is low (Barbour and Hausser, 1997). However, at some synapses, such as the climbing-fiber synapse, desensitization does not contribute to short-term plasticity even though each climbing fiber makes hundreds of synaptic contacts with a Purkinje cell, and the probability of release is high (Dittman et al., 2000; Silver et al., 1998). This is likely a consequence of glial ensheathment of individual sites and the presence of glutamate transporters that isolate release sites and prevent glutamate released from one site from desensitizing AMPAR at neighboring receptor clusters (Dzubay and Jahr, 1999; Otis et al., 1997; Peters et al., 1991; Xu-Friedman et al., 2001). In the case of the climbing-fiber synapse, vesicle fusion at an individual release site may lead to receptor desensitization. However, presynaptic depression, which is longer lived than desensitization (Dittman et al., 2000; Hashimoto and Kano, 1998; Silver et al., 1998), decreases the probability that another vesicle is released from the same site, thus obscuring the effects of desensitization on short-term plasticity. Therefore, for a variety of reasons, desensitization imparts a form of short-term plasticity to the retinogeniculate and calyceal auditory synapses that has not been widely observed at CNS synapses.

NMDAR Saturation at the Retinogeniculate Synapse

A postsynaptic mechanism also contributes to plasticity of the NMDAR response to physiological stimulation patterns. For pairs of pulses at room temperature there is a fast component of recovery from depression. Using a rapidly dissociating antagonist, we demonstrate that this component of synaptic depression reflects NMDAR saturation. Significant saturation also occurs during physiological stimulation, where NMDAR EPSC amplitudes are decreased by up to 3-fold during high-frequency physiological stimulation. NMDAR saturation has also been shown to occur during high-frequency trains at the mouse calyx of Held to medial nucleus of the trapezoid body (MNTB) auditory synapse at room temperature (Wang, 2000).

At the retinogeniculate synapse, the rapidly recovering phase of NMDAR plasticity, like AMPAR plasticity, likely reflects the morphology of this synapse. However, NMDA receptors and AMPA receptors, which have very different properties, respond in distinct ways to the same glutamate signal. Several properties of the NMDAR increase the likelihood of pooled glutamate, causing saturation of neighboring NMDAR. For example, when bound to glutamate, the NMDAR continues to conduct current, while the AMPAR desensitizes. Addi-

tionally, NMDAR has slower kinetics than AMPAR, resulting in a higher probability that an NMDA channel influenced by glutamate from a neighboring site is still in the open state when a subsequent release event occurs.

Physiological Consequences of Synaptic Plasticity

NMDAR saturation and AMPAR desensitization may help to explain the visual responses of relay neurons observed in vivo. In vivo studies have shown that the visual response of relay neurons of the cat LGN can be significantly reduced by iontophoretic application of NMDA-receptor antagonists (Kwon et al., 1991). In some cases, the visual responses in relay cells were nearly eliminated (Heggelund and Hartveit, 1990; Sillito et al., 1990). Moreover, in vitro intracellular voltage recordings in the rat LGN have demonstrated an elimination of the geniculate cell firing response to high-frequency optic nerve stimulation in the presence of inhibitors of NMDARs (Turner et al., 1994). The contribution of the NMDAR in mediating the visual response was surprising because the AMPAR currents appeared to be capable of firing relay neurons with a comfortable safety factor (Chen and Regehr, 2000). However, our findings are consistent with these in vivo and in vitro observations because desensitization during rapid firing of retinal ganglion cells markedly reduces the AMPA current. In some cases, the AMPA component is reduced sufficiently that it no longer fires the postsynaptic cell, as in Turner et al. (1994). Meanwhile, the NMDAR component becomes increasingly prominent during the train and important for the visual responses of relay neurons, and the remaining AMPAR component is likely to contribute by relieving the voltage-dependent block of the NMDAR component. This interplay between NMDAR saturation and AMPAR desensitization may be a general feature of glomerular synapses, such as the mossy fiber to granule cell synapse in the cerebellum, where NMDAR antagonists also inhibit postsynaptic firing produced by high-frequency synaptic activation (D'Angelo et al., 1995).

Relating the properties of retinogeniculate synapses we observe in voltage clamp to the visual responses of relay neurons observed in vivo is complicated by a number of issues. Our study examines synaptic mechanisms in isolation from cortical feedback, brainstem modulatory inputs, intrinsic inhibitory circuitry, and voltage-gated conductances in relay cells, which all help to shape the visual response in vivo (McCormick and Bal, 1994, 1997; Steriade et al., 1997). Although the response of a relay neuron to retinal input depends upon all of these factors, it is likely that AMPAR desensitization and NMDAR saturation contribute to the geniculate neuron response to visual stimuli (Heggelund and Hartveit, 1990; Kwon et al., 1991; Sillito et al., 1990; Turner et al., 1994). However, it is not straightforward to quantify the contributions of receptor desensitization and saturation to postsynaptic firing by assessing the effects of pharmacological manipulations on current clamp recordings. For example, in addition to enhancing the EPSC amplitude, CTZ prolongs the time course of the synaptic current. An alternative approach, which, in the future may improve our understanding of the contributions of these postsynaptic mechanisms, is to simulate retinal inputs with and without AMPAR desensitization and NMDAR saturation with dynamic clamp in a way that is not possible with pharmacological tools (Sharp et al., 1993).

Differences in species, stimulation patterns, and spontaneous activity are also important when relating synaptic properties to in vivo studies. For example, this combination of issues make it difficult to compare our results to in vivo studies that employed rapidly changing visual stimulation and found heightened responses of thalamic relay cells to the second of two closely spaced retinal ganglion cell action potentials (Mastronarde, 1987; Rowe and Fischer, 2001; Usrey et al., 1998). Although our findings suggest that this property does not arise from synaptic facilitation, further experiments will be needed to directly relate our synaptic findings to such in vivo observations.

Previously, it has been shown that the firing pattern of relay neurons is influenced by their intrinsic conductances, the circuitry within the thalamus, modulatory inputs, and feedback from the cortex (Steriade et al., 1997). Here, we show that in addition, during physiological activation, retinogeniculate synapses exhibit short-term plasticity that is mediated by a variety of mechanisms. Presynaptic depression may allow synapses to extend their fidelity over a wide range of firing rates, as has been proposed for cortical synapses (Abbott et al., 1997). Moreover, postsynaptic mechanisms lead to profound changes in synaptic strength in a frequency-dependent manner. These synaptic processes are likely to contribute to the shaping of the relay neuron responses to visual stimulation.

Experimental Procedures

Slice Preparation

Brain slices of the dorsal lateral geniculate nucleus (LGN) were obtained from P25–P32 Black Swiss mice, as previously described (Chen and Regehr, 2000), with slight modification. To increase the number of viable cells, 250 μm slices of the brain were cut in an oxygenated 4°C 2.5% wt/vol. sucrose solution containing: 79 mM NaCl, 23 mM $NaHCO_3$, 68 mM sucrose, 23 mM glucose, 2.3 mM KCl, 1.1 mM NaH_2PO_4, 6.4 mM $MgCl_2$, and 0.45 mM $CaCl_2$. The slices were allowed to recover over 30 min in the sucrose cutting solution at 30°C before they were transferred to a saline solution containing: 125 mM NaCl, 2.5 mM KCl, 2.6 mM NaH_2PO_4, 25 mM glucose, 2 mM $CaCl_2$, and 1 mM $MgCl_2$.

Electrophysiology

Whole-cell voltage clamp recordings from geniculate neurons were obtained using patch pipettes (1.2–2.0 MΩ) containing an internal solution that minimized the contributions of intrinsic membrane conductances and second messenger systems to the synaptic response: 35 mM CsF, 100 mM CsCl, 10 mM EGTA, 10 mM HEPES, 0.1 mM D600 (pH 7.4), as previously described (Chen and Regehr, 2000). The cortex was separated from the thalamus to prevent recurrent excitation between geniculate and cortical neurons. All extracellular recording solutions contained the $GABA_A$ receptor antagonist bicuculline (20 μM, Sigma) to block inhibitory synaptic responses. Paired-pulse experiments were performed at 24°C due to the ease of maintaining a stable patch recording for long periods of time. Studies of the AMPAR or NMDAR component of synaptic current were performed in the presence of CPP (5 μM, Tocris) or NBQX (5 or 10 μM, disodium salt; Tocris), respectively.

The optic tract was stimulated with intensities ranging from 1–40 μA (duration 0.2–0.3 ms) by a pair of saline-filled glass electrodes in bipolar configuration separated by 50–200 μm. Whenever possible, synaptic responses were obtained from single-fiber stimulation, as previously described (Chen and Regehr, 2000). Briefly, the minimal

stimulation intensity was identified using increments of 0.25 μA. In about half the cases (20/44 cells), the stimulus intensity was increased above minimal stimulation if the first input was small, and a second input was identified that was greater than ten times stronger than the first input. The synaptic responses of these multiple inputs were also used. We found that the synaptic responses to low- and high-frequency stimulation at the mouse retinogeniculate connection are extremely reproducible from cell to cell, regardless of the location of the relay neuron.

Experiments involving physiological trains contained $GABA_B$ receptor antagonist, (2S)-3-[[(1S)-1-(3,4-dichlorophenyl)ethyl]amino-2-hydroxypropyl] (phenylmethyl) phosphinic acid (CGP55845, Tocris), and the adenosine receptor antagonist 8-cyclopentyl-1,3-dipropylxanthine (DPCPX, Tocris) in the extracellular solution to prevent activation of endogenous G protein-mediated modulation during train stimuli. Group II and III metabotropic glutamate receptors do not play a significant modulatory role at this connection since the agonists L-CCG-I (2 μM, n = 3 cells; Tocris) and L-AP4 (10 μM, n = 3 cells; Tocris) had no effect on the synaptic response to pairs of pulses (data not shown). Stock solutions of all pharmacological agents, including SDZ ([S]-α-Amino-2′-chloro-5-(phosphonomethyl)[1,1'-biphenyl]-3-propanoic acid), L-AP5, CTZ, NBQX (Tocris) were stored at −20°C and diluted at least 1:1000 to the final concentrations immediately prior to bath application.

To maintain constant bath flow during application of pharmacological agents, a perfusion pump (Gilson) was used at flow rates of 2–3 ml/min for room temperature experiments and 3–4 ml/min for experiments at 34°C–37°C. Recordings at 34°C–37°C were performed using an in-line heater (Warner, CT).

Physiological Trains

The retinal ganglion cell firing pattern used for stimulation was kindly provided by Dr. Sheila Nirenberg, UCLA. The firing pattern was obtained from an ON cell in response to a flash of light that turned on at time 0 and persisted for the length of the pattern used. The optic tract was stimulated with this pattern every 2 min.

Repetitive retinal input stimulation may recruit additional fibers during a train. This is less likely to be an issue in P25–P32 mice because only a few retinal ganglion cells drive a given relay neuron (Chen and Regehr, 2000). Only synaptic responses where an increase in stimulus intensity by ~2.5 to ~5 μA did not recruit additional current were used for experiments involving physiological trains.

Data Acquisition and Analysis

Synaptic currents were acquired with an Axopatch 200B (Axon Instruments) filtered at 1 kHz and digitized at 10–20 kHz with an ITC-16 interface (Instrutech). All off-line data analysis was performed using Igor Pro software (Wavemetrics, OR) and custom macros.

Recovery from depression time courses were obtained by measuring the peak AMPAR or NMDAR EPSCs evoked by pairs of retinal input stimuli. Randomized interstimulus intervals (10, 20, 50, 100, 200, 500, 1000, 2000, 4000, and 8000 ms) were interleaved with a single conditioning pulse. An intertrial interval of 40 s was used to minimize rundown of the NMDA current (Vissel et al., 2001). Averages of three to five trials were used to measure the paired-pulse ratio (A2/A1 × 100) for each ISI. A2 is the peak amplitude of the second EPSC obtained by subtracting the average single conditioning EPSC from the average EPSC response to a pair of stimuli. A1 is the average peak amplitude of the first EPSC. The incremental peak amplitude of each EPSC (A) in a train was measured as the difference between the peak and trough amplitude of the total current after a given stimulus. The relative peak amplitude of the current is then calculated as A/A1 × 100, where A1 is the amplitude of the first EPSC of a train.

Acknowledgments

We thank Sheila Nirenberg for providing the retinal ganglion cell firing pattern used for stimulation and Adam Carter, Solange Brown, Anatol Kreitzer, and Matthew Xu-Friedman for comments on the manuscript. This work was supported by the National Institutes of Health KO8-NS02056 and the Charles H. Hood Foundation to C.C., RO1-NS32405 and P01-NS38312 to W.G.R., and 5 T32 NS07484 to D.M.B.

Received September 19, 2001; revised January 2, 2002.

References

Abbott, L.F., Sen, K., Varela, J.A., and Nelson, S.B. (1997). Synaptic depression and cortical gain control. Science *275*, 220–222.

Barbour, B., and Hausser, M. (1997). Intersynaptic diffusion of neurotransmitter. Trends Neurosci. *20*, 377–384.

Bellingham, M.C., and Walmsley, B. (1999). A novel presynaptic inhibitory mechanism underlies paired pulse depression at a fast central synapse. Neuron *23*, 159–170.

Brenowitz, S., and Trussell, L.O. (2001). Minimizing synaptic depression by control of release probability. J. Neurosci. *21*, 1857–1867.

Cant, N.B., and Morest, D.K. (1979). The bushy cells in the anteroventral cochlear nucleus of the cat. A study with the electron microscope. Neuroscience *4*, 1925–1945.

Chen, C., and Regehr, W.G. (2000). Developmental remodeling of the retinogeniculate synapse. Neuron *28*, 955–966.

Chen, C.Y., Horowitz, J.M., and Bonham, A.C. (1999). A presynaptic mechanism contributes to depression of autonomic signal transmission in NTS. Am. J. Physiol. *277*, H1350–H1360.

Cleland, B.G., and Lee, B.B. (1985). A comparison of visual responses of cat lateral geniculate nucleus neurones with those of ganglion cells afferent to them. J. Physiol. (Lond.) *369*, 249–268.

Clements, J.D., Lester, R.A., Tong, G., Jahr, C.E., and Westbrook, G.L. (1992). The time course of glutamate in the synaptic cleft. Science *258*, 1498–1501.

D'Angelo, E., De Filippi, G., Rossi, P., and Taglietti, V. (1995). Synaptic excitation of individual rat cerebellar granule cells in situ: evidence for the role of NMDA receptors. J. Physiol. (Lond.) *484*, 397–413.

Diamond, J.S., and Jahr, C.E. (1995). Asynchronous release of synaptic vesicles determines the time course of the AMPA receptor-mediated EPSC. Neuron *15*, 1097–1107.

Dittman, J.S., and Regehr, W.G. (1998). Calcium dependence and recovery kinetics of presynaptic depression at the climbing fiber to Purkinje cell synapse. J. Neurosci. *18*, 6147–6162.

Dittman, J.S., Kreitzer, A.C., and Regehr, W.G. (2000). Interplay between facilitation, depression, and residual calcium at three presynaptic terminals. J. Neurosci. *20*, 1374–1385.

Dzubay, J.A., and Jahr, C.E. (1999). The concentration of synaptically released glutamate outside of the climbing fiber-Purkinje cell synaptic cleft. J. Neurosci. *19*, 5265–5274.

Famiglietti, E.V., Jr., and Peters, A. (1972). The synaptic glomerulus and the intrinsic neuron in the dorsal lateral geniculate nucleus of the cat. J. Comp. Neurol. *144*, 285–334.

Guido, W., and Lu, S.M. (1995). Cellular bases for the control of retinogeniculate signal transmission. Int. J. Neurosci. *80*, 41–63.

Hamos, J.E., Van Horn, S.C., Raczkowski, D., Uhlrich, D.J., and Sherman, S.M. (1985). Synaptic connectivity of a local circuit neurone in lateral geniculate nucleus of the cat. Nature *317*, 618–621.

Hamos, J.E., Van Horn, S.C., Raczkowski, D., and Sherman, S.M. (1987). Synaptic circuits involving an individual retinogeniculate axon in the cat. J. Comp. Neurol. *259*, 165–192.

Hashimoto, K., and Kano, M. (1998). Presynaptic origin of paired-pulse depression at climbing fibre-Purkinje cell synapses in the rat cerebellum. J. Physiol. (Lond.) *506*, 391–405.

Heggelund, P., and Hartveit, E. (1990). Neurotransmitter receptors mediating excitatory input to cells in the cat lateral geniculate nucleus. I. Lagged cells. J. Neurophysiol. *63*, 1347–1360.

Hestrin, S. (1992). Activation and desensitization of glutamate-activated channels mediating fast excitatory synaptic currents in the visual cortex. Neuron *9*, 991–999.

Hjelmstad, G.O., Isaac, J.T., Nicoll, R.A., and Malenka, R.C. (1999). Lack of AMPA receptor desensitization during basal synaptic transmission in the hippocampal slice. J. Neurophysiol. *81*, 3096–3099.

Kinney, G.A., Overstreet, L.S., and Slater, N.T. (1997). Prolonged physiological entrapment of glutamate in the synaptic cleft of cerebellar unipolar brush cells. J. Neurophysiol. *78*, 1320–1333.

Kwon, Y.H., Esguerra, M., and Sur, M. (1991). NMDA and non-NMDA receptors mediate visual responses of neurons in the cat's lateral geniculate nucleus. J. Neurophysiol. *66*, 414–428.

Lenn, N.J., and Reese, T.S. (1966). The fine structure of nerve endings in the nucleus of the trapezoid body and the ventral cochlear nucleus. Am. J. Anat. *118*, 375–389.

Magleby, K.L. (1987). Short-term changes in synaptic efficacy. In Synaptic Function, G.M. Edelman, W.E. Gall, and W.M. Cowan, eds. (New York: John Wiley & Sons), pp. 21–56.

Mastronarde, D.N. (1987). Two classes of single-input X-cells in cat lateral geniculate nucleus. II. Retinal inputs and the generation of receptive-field properties. J. Neurophysiol. *57*, 381–413.

Mastronarde, D.N. (1992). Nonlagged relay cells and interneurons in the cat lateral geniculate nucleus: receptive-field properties and retinal inputs. Vis. Neurosci. *8*, 407–441.

McCormick, D.A., and Bal, T. (1994). Sensory gating mechanisms of the thalamus. Curr. Opin. Neurobiol. *4*, 550–556.

McCormick, D.A., and Bal, T. (1997). Sleep and arousal: thalamocortical mechanisms. Annu. Rev. Neurosci. *20*, 185–215.

Oleskevich, S., Clements, J., and Walmsley, B. (2000). Release probability modulates short-term plasticity at a rat giant terminal. J. Physiol. (Lond.) *524*, 513–523.

Olverman, H.J., Jones, A.W., and Watkins, J.C. (1988). [3H]D-2-amino-5-phosphonopentanoate as a ligand for N-methyl-D-aspartate receptors in the mammalian central nervous system. Neuroscience *26*, 1–15.

Otis, T., Zhang, S., and Trussell, L.O. (1996a). Direct measurement of AMPA receptor desensitization induced by glutamatergic synaptic transmission. J. Neurosci. *16*, 7496–7504.

Otis, T.S., Wu, Y.C., and Trussell, L.O. (1996b). Delayed clearance of transmitter and the role of glutamate transporters at synapses with multiple release sites. J. Neurosci. *16*, 1634–1644.

Otis, T.S., Kavanaugh, M.P., and Jahr, C.E. (1997). Postsynaptic glutamate transport at the climbing fiber-Purkinje cell synapse. Science *277*, 1515–1518.

Parks, T.N. (1981). Morphology of axosomatic endings in an avian cochlear nucleus: nucleus magnocellularis of the chicken. J. Comp. Neurol. *203*, 425–440.

Peters, A., Palay, S.L., and Webster, H. (1991). The Fine Structure of the Nervous System: Neurons and Their Supporting Cells, Third Edition (New York: Oxford University Press).

Raman, I.M., Zhang, S., and Trussell, L.O. (1994). Pathway-specific variants of AMPA receptors and their contribution to neuronal signaling. J. Neurosci. *14*, 4998–5010.

Ramoa, A.S., and McCormick, D.A. (1994). Enhanced activation of NMDA receptor responses at the immature retinogeniculate synapse. J. Neurosci. *14*, 2098–2105.

Rowe, M.H., and Fischer, Q. (2001). Dynamic properties of retinogeniculate synapses in the cat. Vis. Neurosci. *18*, 219–231.

Sharp, A.A., O'Neil, M.B., Abbott, L.F., and Marder, E. (1993). Dynamic clamp: computer-generated conductances in real neurons. J. Neurophysiol. *69*, 992–995.

Sherman, S.M., and Guillery, R.W. (1996). Functional organization of thalamocortical relays. J. Neurophysiol. *76*, 1367–1395.

Sillito, A.M., Murphy, P.C., Salt, T.E., and Moody, C.I. (1990). Dependence of retinogeniculate transmission in cat on NMDA receptors. J. Neurophysiol. *63*, 347–355.

Silver, R.A., Cull-Candy, S.G., and Takahashi, T. (1996). Non-NMDA glutamate receptor occupancy and open probability at a rat cerebellar synapse with single and multiple release sites. J. Physiol. (Lond.) *494*, 231–250.

Silver, R.A., Momiyama, A., and Cull-Candy, S.G. (1998). Locus of frequency-dependent depression identified with multiple-probability fluctuation analysis at rat climbing fibre-Purkinje cell synapses. J. Physiol. (Lond.) *510*, 881–902.

Steriade, M., Jones, E.G., and McCormick, D.A. (1997). Thalamus (Oxford: Elsevier Science Ltd).

Trussell, L.O. (1997). Cellular mechanisms for preservation of timing in central auditory pathways. Curr. Opin. Neurobiol. *7*, 487–492.

Trussell, L.O. (1999). Synaptic mechanisms for coding timing in auditory neurons. Annu. Rev. Physiol. *61*, 477–496.

Trussell, L.O., Zhang, S., and Raman, I.M. (1993). Desensitization of AMPA receptors upon multiquantal neurotransmitter release. Neuron *10*, 1185–1196.

Turner, J.P., and Salt, T.E. (1998). Characterization of sensory and corticothalamic excitatory inputs to rat thalamocortical neurones in vitro. J. Physiol. (Lond.) *510*, 829–843.

Turner, J.P., Leresche, N., Guyon, A., Soltesz, I., and Crunelli, V. (1994). Sensory input and burst firing output of rat and cat thalamocortical cells: the role of NMDA and non-NMDA receptors. J. Physiol. (Lond.) *480*, 281–295.

Urwyler, S., Laurie, D., Lowe, D.A., Meier, C.L., and Muller, W. (1996). Biphenyl-derivatives of 2-amino-7-phosphonoheptanoic acid, a novel class of potent competitive N-methyl-D-aspartate receptor antagonist—I. Pharmacological characterization in vitro. Neuropharmacology *35*, 643–654.

Usrey, W.M., and Reid, R.C. (1999). Synchronous activity in the visual system. Annu. Rev. Physiol. *61*, 435–456.

Usrey, W.M., Reppas, J.B., and Reid, R.C. (1998). Paired-spike interactions and synaptic efficacy of retinal inputs to the thalamus. Nature *395*, 384–387.

Vissel, B., Krupp, J.J., Heinemann, S.E., and Westbrook, G.L. (2001). A use-dependent tyrosine dephosphorylation of NMDA receptors is independent of ion flux. Nat. Neurosci. *4*, 587–596.

Walmsley, B., Alvarez, F.J., and Fyffe, R.E. (1998). Diversity of structure and function at mammalian central synapses. Trends Neurosci. *21*, 81–88.

Wang, L.Y. (2000). The dynamic range for gain control of NMDA receptor-mediated synaptic transmission at a single synapse. J. Neurosci. *20*, RC115.

Wilson, J.R., Friedlander, M.J., and Sherman, S.M. (1984). Fine structural morphology of identified X- and Y-cells in the cat's lateral geniculate nucleus. Proc. R. Soc. Lond. B Biol. Sci. *221*, 411–436.

Xu-Friedman, M.A., Harris, K.M., and Regehr, W.G. (2001). Three-dimensional comparison of ultrastructural characterization of depressing and facilitating synapses onto cerebellar Purkinje cells. J. Neurosci. *21*, 6666–6672.

Zucker, R.S. (1989). Short-term synaptic plasticity. Annu. Rev. Neurosci. *12*, 13–31.

Zucker, R.S. (1999). Calcium- and activity-dependent synaptic plasticity. Curr. Opin. Neurobiol. *9*, 305–313.